Thermal seasons in northern Europe in projected future climate

Ruosteenoja, Kimmo

2020-08

Ruosteenoja , K , Markkanen , T & Räisänen , J 2020 , ' Thermal seasons in northern Europe in projected future climate ' , International Journal of Climatology , vol. 40 , no. 10 , pp. 4444-4462 . https://doi.org/10.1002/joc.6466

http://hdl.handle.net/10138/318615
https://doi.org/10.1002/joc.6466

Received: 28 October 2019 | Revised: 23 December 2019 | Accepted: 26 December 2019 | Published on: 14 January 2020

DOI: 10.1002/joc.6466

RESEARCH ARTICLE

International Journal of Climatology RMetS

Thermal seasons in northern Europe in projected future climate

Kimmo Ruosteenoja[1] | **Tiina Markkanen**[1] | **Jouni Räisänen**[2]

[1]Finnish Meteorological Institute, Helsinki, Finland

[2]Department of Physics, University of Helsinki, Helsinki, Finland

Correspondence
Kimmo Ruosteenoja, Finnish Meteorological Institute, P.O. Box 503, FI-00101 Helsinki, Finland.
Email: kimmo.ruosteenoja@fmi.fi

Funding information
Academy of Finland, Grant/Award Numbers: 312932, 314224

Abstract

Global warming acts to prolong thermal summers and shorten winters. In this work, future changes in the lengths and timing of four thermal seasons in northern Europe, with threshold temperatures 0 and 10°C, are derived from bias-adjusted output data from 23 CMIP5 global climate models. Three future periods and two Representative Concentration Pathway (RCP) scenarios are discussed. The focus is on the period 2040–2069 under RCP4.5, which approximately corresponds to a 2°C global warming relative to the preindustrial era. By the period 2040–2069, the average length of the thermal summer increases by nearly 30 days relative to 1971–2000, and the thermal winter shortens by 30–60 days. The timing of the thermal springs advances while autumns delay. Within the model ensemble, there is a high linear correlation between the modelled annual-mean temperature increase and shifts in the thermal seasons. Thermal summers lengthen by about 10 days and winters shorten by 10–24 days per 1°C of local warming. In the mid-21st century, about two-thirds of all summers (winters) are projected to be very long (very short) according to the baseline-period standards, with an anomaly greater than 20 days relative to the late-20th century temporal mean. The proportion of years without a thermal winter increases remarkably in the Baltic countries and southern Scandinavian peninsula. Implications of the changing thermal seasons on nature and human society are discussed in a literature review.

KEYWORDS

2°C global warming target, bias correction, climate change, representative concentration pathways (RCPs), temperature deviation integral method, thermal summer, thermal winter

1 | INTRODUCTION

Ongoing global warming leads to a prolongation of thermal summers and shortening of thermal winters. In this article, quantitative projections for the lengths and onset dates of four thermal seasons in northern Europe are inferred from global climate model (GCM) simulations performed within the context of Phase 5 of the Coupled Model Intercomparison Project (CMIP5). In addition to the time-mean changes, temporal variability and probabilities for the occurrence of anomalously long and short thermal seasons are considered.

According to the definition applied in the present work, the thermal winter consists of that part of the year

when the daily mean temperature is below 0°C. During the thermal summer, the mean temperatures exceed 10°C, while in the intermediate seasons, temperatures fall between the two threshold values. These threshold temperatures are used in Finland (Ruosteenoja *et al.*, 2011), Norway (https://snl.no/sommer) and Sweden (https://www.smhi.se/kunskapsbanken/meteorologi/arstider-1.1082). The definitions confine the analysis to northern Europe, since elsewhere in Europe the temperature thresholds applied for summer are commonly higher: for example, +13°C in the former Soviet Union (Jaagus *et al.*, 2003) and +15°C in Poland (Czernecki and Miętus, 2017); in both works, the temperature limit for the thermal winter is 0°C. To mention a more peculiar example, in Arctic areas the generally applied thresholds for the thermal winter and summer are −2.5 and +2.5°C, respectively (Przybylak and Wyszyński, 2017, and references therein).

In some studies, the definitions of the thermal seasons are spatially varying, without any universal temperature limits (e.g. Peña-Ortiz *et al.*, 2015; Allen and Sheridan, 2016; Park *et al.*, 2018). For example, in Park *et al.* (2018) the thermal summer encompasses the quarter of year that is warmest according to local long-term temperature records. Such an approach is reasonable when one studies the thermal seasons over a continental domain containing highly divergent climates.

Changes in the lengths and timing of the thermal seasons have many impacts on nature and human society. For example, ice season in seas and watersheds shortens and spring floods become earlier. For some animal species, the consequences may even be disastrous. Potential impacts of the changing thermal seasons are discussed in more detail in the literature review in Section 5.

Long-term past changes in the thermal seasons have been documented in several observation-based studies. In the European part of the former Soviet Union during the period 1881–1995, Jaagus *et al.* (2003) reported a widespread shortening of the thermal winter by 1–2 weeks. In particular, the termination of the winter has advanced. In southern Estonia, the durations of summer and winter changed by +11 and −29 days, respectively, between 1891 and 2003 (Kull *et al.*, 2008). In Poland, according to a trend fitted to observations for the period 1951–2010, the thermal winter has shortened by nearly 40 days and summer lengthened by nearly 20 days (Czernecki and Miętus, 2017). Simultaneously, years without a thermal winter have become more frequent. Considering an All-European average for the period 1950–2012, Peña-Ortiz *et al.* (2015) reported a lengthening of the thermal summers by 2.4 days per decade, on average; however, the bulk of the lengthening has taken place after 1979.

In Novaya Zemlya, in the latest normal period 1981–2010 thermal summers have been 30–50 days longer than in the late 19th and early 20th century (Przybylak and Wyszyński, 2017). Meanwhile, the thermal winter and spring have both shortened by 20–30 days. In the United States, in exploring nationwide average, summers have lengthened by 19 and winters shortened by 25 days between 1948 and 2012 (Allen and Sheridan, 2016). In eastern China, the thermal summer extended by 12 days between 1961 and 2007 (Yang *et al.*, 2013). In Argentina, 18 meteorological stations out of 39 showed a statistically significant positive trend in the thermal summer length during the period 1940–2007 (Fernández-Long *et al.*, 2013). Considering the entire extratropical continental area of the Northern Hemisphere, Park *et al.* (2018) reported an average increase of 25 days in the summer length in 1953–2012 (using a spatially dependent definition for the summer, see above). The largest increment has taken place in Europe, while in central United States summers have even become shorter. As discussed above, the definitions of thermal seasons diverge among the studies, and therefore the trends reported are not directly comparable.

Future projections of the thermal seasons have been discussed in literature far less widely than the observed trends. Ruosteenoja *et al.* (2011) produced such projections for Finland by utilizing 19 CMIP3 GCMs; under the B1 scenario, the thermal summer was projected to be prolonged by 20–30 days and winter reduced by 30–90 days by the late-21st century. In China, according to a mean of five GCMs and an average over the country, the lengthening of the thermal summer by 2071–2099 ranges from 16 to 50 days across the four Representative Concentration Pathway (RCP) scenarios (Deng *et al.*, 2018), even though the lengthening is strongly spatially dependent, as also shown in the earlier study of Tian *et al.* (2014). On the other hand, projections for the thermal growing season with a base temperature of +5°C have been published for multiple regions, for example, for Norway (Engen-Skaugen and Tveito, 2004), Czechia and Austria (Trnka *et al.*, 2011), Estonia (Saue and Käremaa, 2015), the entire European area (Ruosteenoja *et al.*, 2016) and northern Eurasia (Zhou *et al.*, 2018).

In the present article, projections for the durations and start dates of the thermal seasons presented in Ruosteenoja *et al.* (2011) are updated to correspond to the CMIP5 simulations and Representative Concentration Pathways (RCPs) and extended geographically to cover the whole northern Europe. Unlike in that study, in the present work the onset and end dates of the thermal seasons are derived from bias-corrected daily model output data instead of monthly data. Besides, in addition to time-mean changes, we explore temporal variations and the occurrence of very short and long thermal seasons.

The article first introduces the model data and the determination of the start and termination dates of the thermal seasons (Section 2). Thereafter, we explore time-mean

changes in the timing and duration of the seasons and the relation between these changes and the modelled increase in the annual-mean temperature (Section 3). Section 4 deals with the temporal variability in the season lengths and, in particular, the occurrence of anomalous thermal seasons (e.g. years without a thermal winter or with an exceptionally long thermal summer). Implications of the projected changes are discussed in Section 5, and the main conclusions of the work are summarized in Section 6.

2 | MODEL DATA AND DETERMINATION OF THE ONSET DATES

The CMIP5 models analysed in this work are listed in Table 1. Projections for RCP4.5 are derived from 23, those for RCP8.5 from 22 GCMs. In Luomaranta *et al.* (2014), 28 CMIP5 GCMs were identified that are able to simulate northern European current climate and past temperature trends reasonably. The bias correction procedure requires model output data at daily temporal resolution, which further excludes five (for RCP8.5, six) GCMs. Ten GCMs provide data from more than one parallel run for either or both the RCP scenarios (Table 1). Parallel runs are utilized in the present work to improve the robustness of the analyses.

TABLE 1 Global climate models used in this work

Model	$N_{4.5}$	$N_{8.5}$	$\Delta T_{4.5}$	$\Delta T_{8.5}$
MIROC5	3	3	3.1	3.8
MIROC-ESM	1	1	3.9	4.7
MIROC-ESM-CHEM	1	1	3.9	4.9
MRI-CGCM3	1	1	1.7	2.9
BCC-CSM1-1	1	1	2.5	3.7
INMCM4	1	1	1.3	1.8
NorESM1-M	1	1	2.6	3.2
HadGEM2-ES	4	4	3.2	4.2
HadGEM2-CC	1	3	3.0	4.5
MPI-ESM-LR	3	3	1.9	2.7
MPI-ESM-MR	3	1	2.1	2.7
CNRM-CM5	1	1	2.6	3.1
IPSL-CM5A-LR	4	4	3.8	4.9
IPSL-CM5A-MR	1	1	3.0	3.5
CMCC-CM	1	1	3.8	4.5
CMCC-CMS	1	1	4.2	4.4
GFDL-CM3	2	1	3.6	4.9
GFDL-ESM2M	1	1	2.3	2.5
GISS-E2-R	1	–	2.2	–
NCAR-CCSM4	3	3	1.9	2.6
CanESM2	5	5	3.3	4.2
ACCESS1-0	1	1	1.9	3.3
EC-EARTH	3	2	2.0	2.5

Note: Columns 2 and 3 show the count of parallel runs (N) for each model and columns 4 and 5 the annual-mean temperature response ΔT (for models with several parallel runs their mean) from 1971–2000 to 2040–2069 averaged over the northern European land areas (54–72°N, 4–36°E), both given separately for the RCP4.5 and RCP8.5 scenarios.

The GCM simulations do not reproduce the observed temperature climate perfectly, and any bias in the simulated temperatures would distort the timing of the resulting thermal seasons, both the baseline values and future trends. Therefore, bias correction has been performed prior to the actual analyses; the procedure is described in Räisänen and Räty (2013) and applied to the present model ensemble in Ruosteenoja *et al.* (2016) (see their eq. 1). After the correction, both the baseline-period temporal mean and *SD* of the simulated temperatures are close to their observational counterparts. Furthermore, modelled changes in the mean temperature between the baseline and future periods are preserved.

The bias correction procedure requires an observational calibration dataset; for this purpose, the E-OBS analyses (Haylock *et al.*, 2008) are used. The E-OBS analyses are represented on a $0.25 \times 0.25^\circ$ latitude-longitude grid, and bias correction improves the fairly coarse spatial resolution of the GCM output data to the same level. This has been demonstrated in fig. 1 of Ruosteenoja *et al.* (2016). Consequently, the resulting spatial resolution is similar to that in several regional climate models. However, bias correction produces high-resolution data for all the GCMs, and there is no need to restrict the analysis to such a limited GCM ensemble for which dynamical downscalings are available. As a disadvantage, bias correction does not take into consideration the potential dependence of the simulated warming on height. Moreover, the E-OBS analyses only encompass land areas.

For the determination of the onset dates of the thermal seasons, we use the temperature deviation integral method. The same method was utilized in Ruosteenoja *et al.* (2016) to infer the duration of the thermal growing season, and a detailed description of the procedure is given in section 2.2 of that paper. By selecting the appropriate threshold temperatures, the approach can readily be modified to find the onset times of the thermal seasons; these are determined separately for every single year of the model simulation. The advantage of the method is that the start of the thermal spring/summer is not spuriously triggered by a transient early warm episode if this is followed by an intense cold wave (see fig. 2 of Ruosteenoja *et al.* (2016)). Analogously, a sporadic early cool period does not induce the beginning of the thermal autumn or winter.

In the boreal zone, the coldest winter temperatures are generally well below 0°C and mid-summer temperatures above +10°C, and consequently thermal seasons can be determined unequivocally. Problems arise when the threshold values fall close to the minima or maxima of the annual temperature cycle. Thermal winter is regarded as missing if the time interval between the crossings of 0°C is shorter than 3 weeks or the negative temperature sum accumulating between the crossing dates is smaller than 10° days. Such a situation is quite common in Denmark and on the western coasts of Norway, and the area expands as global warming proceeds. For missing winters, the length of the winter is assigned to zero, and the start of the thermal spring and the end of the previous autumn are both set to 25 January; considering the entire domain, this time approximately corresponds to the coldest point of the year. A missing thermal summer is defined analogously: The time interval with the daily mean temperatures above 10°C is shorter than 3 weeks or the temperature sum above 10°C is smaller than 10° days. The thermal spring is then defined to end and the thermal autumn to begin on 21 July. Missing thermal summers occur in the northernmost areas of the domain and over the Scandinavian mountain range, but their frequency declines in the course of the projection time.

The condition that the thermal winter (and summer) should last at least 3 weeks is applied to minimize the occurrence of occasions in which the determination of the thermal season is ambiguous. In mild climate, there frequently occurs several rather short frost periods during the cold part of the year, interspersed by thaw periods. If the acceptable minimum length for the thermal winter were substantially shorter than 3 weeks (e.g. 5 or 10 days), it would be difficult to select which of these several 'micro-winters' should be the 'official' thermal winter. In any case, the criteria for the existence of a thermal summer and winter are ineluctably somewhat arbitrary. If a more or a less stringent definition were employed, the probabilities of missing seasons (Section 4.2) would be to some extent different.

Projections are calculated with respect to the baseline period 1971–2000. We hereby follow the recommendations of WMO (1989) to use a 30-year-long period to calculate climatological standard normals. As the simulations performed under the various RCP scenarios diverge since 2006, this is the latest standard tridecadal period for which the baseline means can be calculated unambiguously.

Future projections are produced primarily for the RCP4.5 scenario that represents moderately large emissions of greenhouse gases (van Vuuren *et al.*, 2011). We particularly focus on the period 2040–2069 which, considering the multi-model mean response to RCP4.5, approximately corresponds to a 2°C global warming relative to the preindustrial climate (Collins *et al.*, 2013, fig. 12.5). Recall, however, that in northern Europe warming exceeds the global mean substantially; even considering the difference between the periods 1971–2000 and 2040–2069 under RCP4.5, 17 GCMs out of 23 simulate a regional temperature increase larger than 2°C (Table 1). Two other projection periods, 2010–2039 and 2070–2099, are discussed as well. For a sensitivity assessment, the supplement file provides some projections for the RCP8.5 scenario; admittedly, climate change estimates produced by this high-emission scenario are quite far from the targets of current climate policy. RCP2.6 and 6.0 are not considered because of the fairly small number of GCMs providing daily data.

To find out the long-term mean onset dates, we first calculated the 30-year means of the dates for each individual model run, and these were utilized to obtain averages over the available parallel runs (Table 1). The multi-model means were then derived from these multi-parallel run means by giving equal weights for all the GCMs, with the exception of MIROC-ESM and MIROC-ESM-CHEM which were weighted by 1/2. Hereby, we avoided giving a summed weight larger than 2 for any individual modelling centre. Leduc *et al.* (2016) have shown that GCMs originating from the same centre tend to produce more similar projections than GCMs in general, thus being less independent of one another.

The resulting multi-model mean onset times of the four thermal seasons for the baseline period are depicted in Figure 1a–d. Thanks to the bias correction, the dates are mainly close to those inferred directly from the E-OBS data. In the Baltic countries and southern Scandinavia, however, the average length of the thermal winter in 1971–2000 proved to be 5–20 days smaller in the E-OBS analyses than in the bias-corrected multi-model mean data. This is largely explained by a period of mild winters that occurred between the years 1988 and 2000; this resulted in an anomalously large proportion of years without a proper thermal winter in these areas. As will be discussed in the next paragraph, in this respect the large bias-corrected GCM dataset evidently represents the baseline-period climate more robustly than the 30-year-long observational time series.

In calculating probabilities for the occurrence of anomalous thermal seasons (e.g. a thermal summer more than 20 days longer than the average over the baseline period), all the model output data are pooled, that is, treated as a single sample. This is feasible since, owing to the bias correction, all the model runs describe the same baseline-period climate (with the mean and *SD* of the temperature consistent with their observational counterparts) but are independent of one another in the evolution of yearly weather conditions. As the total count of parallel runs for RCP4.5 is 44 (Table 1), the model runs

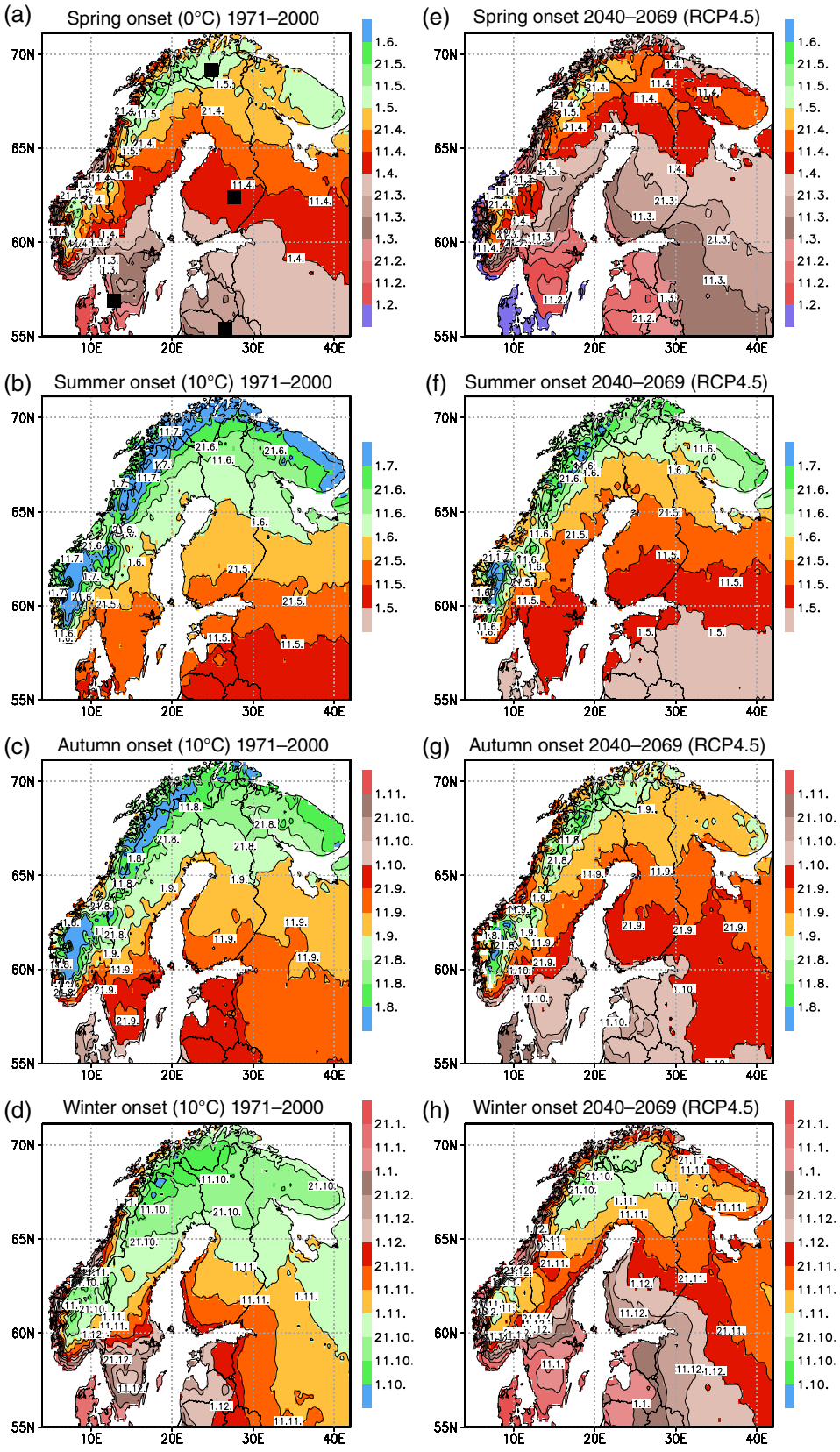

FIGURE 1 Average onset dates of the thermal (a) spring, (b) summer, (c) autumn and (d) winter for the period 1971–2000; the mean of the 23 GCMs. Corresponding onset dates for the period 2040–2069 under RCP4.5 are depicted in panels (e)–(h). The positions of the four grid points examined in the more detailed analyses below are marked by squares in panel (a)

thus constitute a 1,320-year-long time series describing the climate of the period 1971–2000. From such a large sample, one can calculate the probabilities of anomalous seasons (e.g. an exceptionally long thermal summer) with a far higher robustness than from the corresponding 30-year-long observational data. When calculating the

probabilities, each individual model run was weighted by the inverse of the total count of the parallel runs available for that particular model.

For the scenario periods, probabilities for anomalous thermal seasons were calculated from the pooled data in the same manner. Hence, the resulting probabilities encompass both the influence of interannual variability and the different magnitude of warming simulated by the various models.

3 | PROJECTED CHANGES IN THE MEAN ONSET TIMES AND LENGTHS

3.1 | Multi-model means and inter-model differences

Temporally averaged onset times of the thermal seasons for the periods 1971–2000 and 2040–2069 under RCP4.5, corresponding to the mean of the 23 GCMs, are shown in Figure 1. A wider collection of the beginning dates is given in Figures S1–S4, covering the three future time spans and both RCP scenarios.

By mid-century, the start and termination of the thermal summer are projected to become by about 2 weeks earlier and later, respectively. For example, in the Baltic countries, southern Sweden and on the southern coast of Finland, the average thermal summer ends in late September in 1971–2000 (Figure 1c), but by the period 2040–2069 the termination is delayed to the first half of October (Figure 1g). In the very coldest areas (Scandinavian mountains, northern Lapland and the coasts of the Arctic Ocean) the shifts are even larger, the thermal summer lengthening by more than 30 days (Figure 2b).

Concurrently, the start and end dates of the thermal winter are projected to become later and earlier by about 15 days in northern inland areas, while the shifts amount to 30 days near the coasts of the Arctic Ocean and the Baltic Sea between 58°N and 63°N. Accordingly, the thermal winter shortens by 30–60 days (Figure 2d). In the Baltic countries and southern Scandinavian peninsula, the thermal spring is projected to start in February (Figure 1e) rather than in March (Figure 1a). In Denmark and southernmost Sweden, the average winter is already quite short in the baseline-period climate, leaving little room for further shortening.

In the zone extending from the southern Scandinavian peninsula to the Baltic countries and southern Finland, the thermal winter shortens much more than the thermal summer lengthens. In these areas, the thermal spring and autumn are projected to prolongate by more than 10 days (Figure 2a–c). In Denmark and the northern

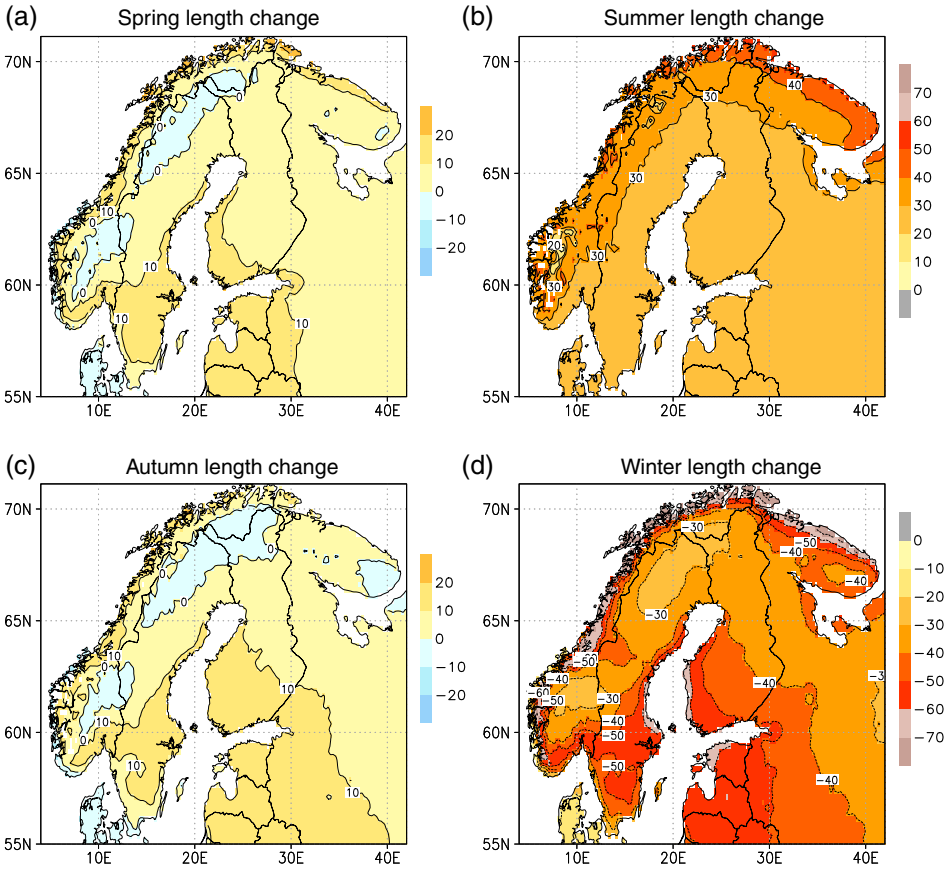

FIGURE 2 Projected multi-model mean changes (in days) in the length of the thermal (a) spring, (b) summer, (c) autumn and (d) winter from the period 1971–2000 to 2040–2069 under RCP4.5

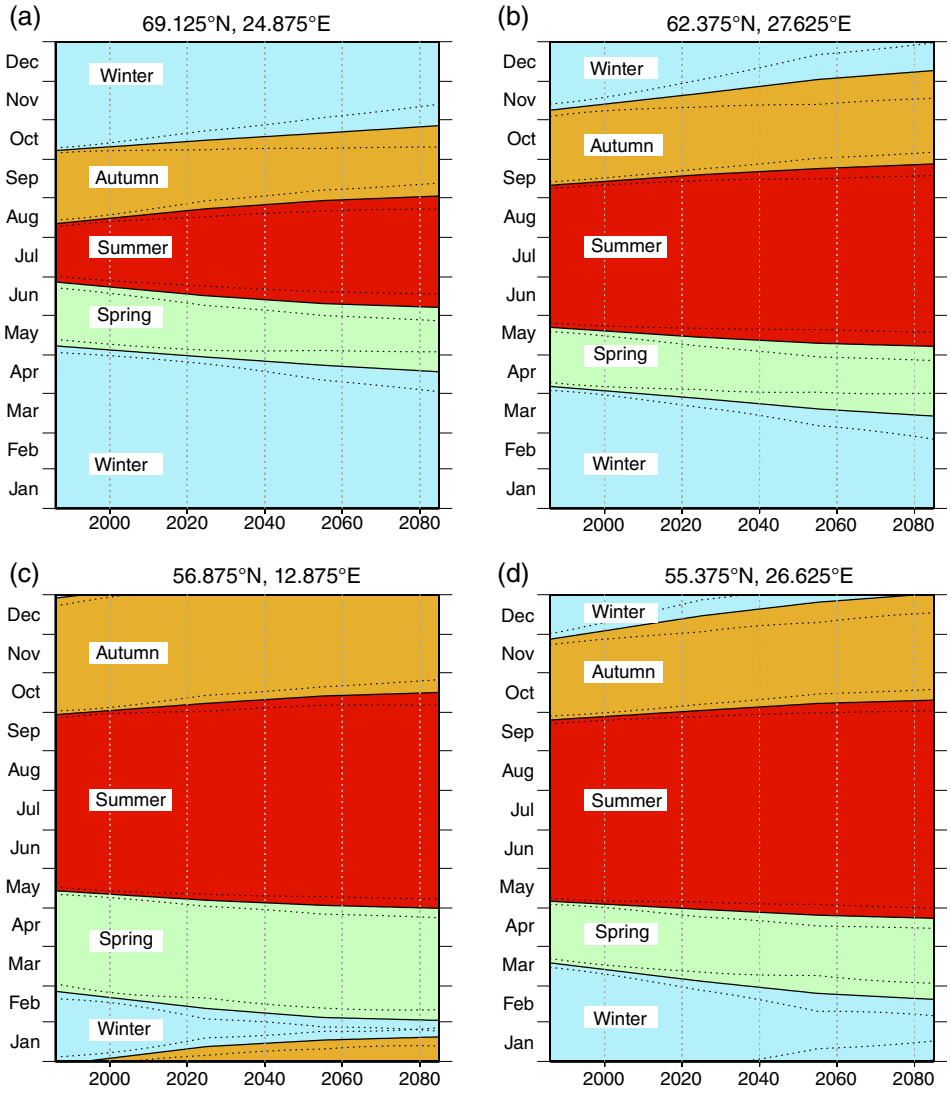

FIGURE 3 Temporal evolution of the average onset times and durations of the thermal seasons under RCP4.5 at four grid points: (a) 69.125°N, 24.875°E, (b) 62.375°N, 27.625°E, (c) 56.875°N, 12.875°E and (d) 55.375°N, 26.625°E; the positions are marked in Figure 1a. On the *x*-axis given are the mid-point years of the 30-year periods (e.g. 1986 refers to the period 1971–2000 and 2085 to 2070–2099). The multi-model mean onset times are denoted by solid lines and the 90% inter-model uncertainly intervals by dotted lines

Fennoscandian inland, the durations of the intermediate seasons remain nearly unchanged.

To illustrate the temporal evolution, Figure 3 depicts the time series of the onset times and lengths of the thermal seasons at four grid points; the dates have first been calculated for the four tridecadal periods and then interpolated linearly in time. To demonstrate inter-model differences, we also show the 90% uncertainty intervals inferred from a normal distribution fitted to the distribution of the responses produced by the 23 GCMs (multi-model mean $\pm$ 1.645 $\times$ inter-model *SD*).

According to Figure 3, trends in the season lengths are steeper in the first than in the second half of the ongoing century. This is in accordance with a deceleration of the RCP4.5-induced global warming during the late-21st century (Collins *et al*., 2013, fig. 12.5). Nonetheless, near the end of the century the projection depends materially on the future emissions of greenhouse gases, RCP8.5 yielding substantially stronger responses than RCP4.5 (Figures S1–S4 and S5–S6).

At the beginning of the period studied, the bias-adjusted data represent the same climate for all GCMs, and therefore in the early years inter-model scatter in the onset dates is small (Figure 3). Later in this century, differences between the models tend to increase. At the end of the 21st century, the uncertainty intervals for the start and end dates of the thermal winter range from 4 to 6 weeks at the inland points and are about 2 weeks on the south-western coast of Sweden. For the onset and termination of the thermal summer, the corresponding uncertainty intervals are 2–3 weeks.

To obtain a deeper insight into the uncertainty of the projections, we calculated inter-model *SD* for the changes in the thermal season lengths (Figure 4). For the lengths of the thermal spring, summer and autumn, the *SD*s across the simulated responses are typically ~10 days, for the thermal winter 10–25 days. However, on the coasts of the Arctic Ocean the responses produced by the individual GCMs diverge to a greater extent than elsewhere. One factor that acts to increase the degree of uncertainty in this

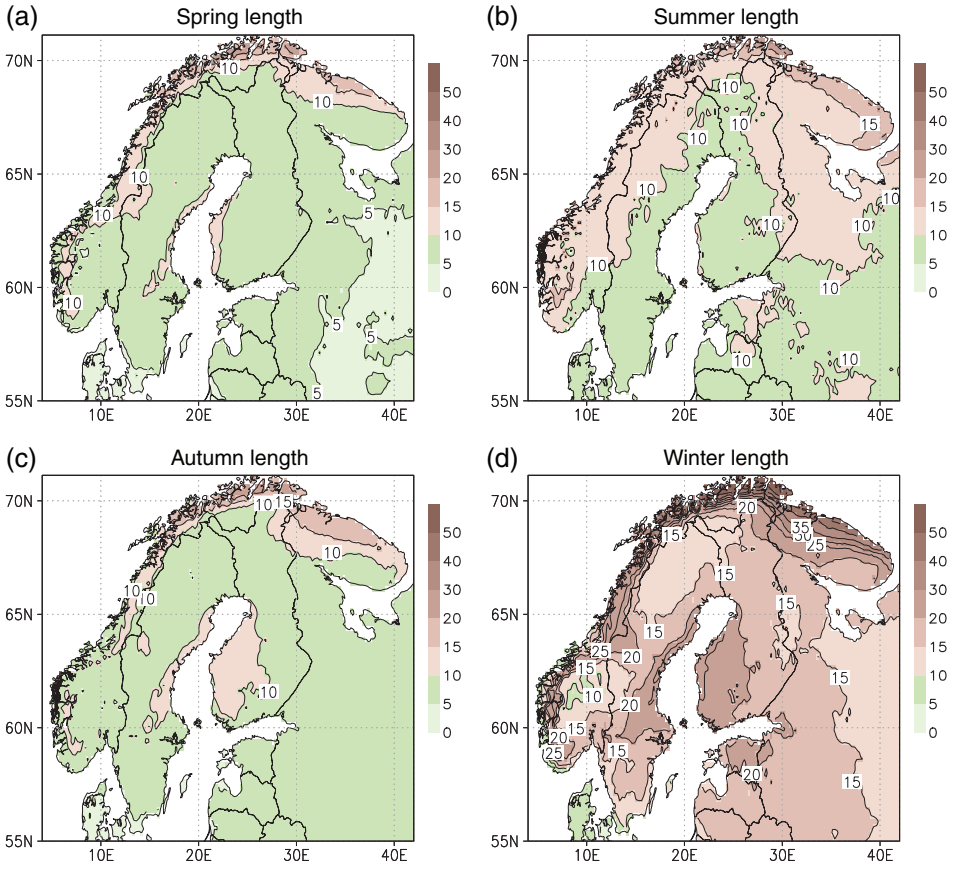

FIGURE 4 Inter-model *SD* of changes in the thermal season lengths (in days) from 1971–2000 to 2040–2069 under RCP4.5: (a) spring, (b) summer, (c) autumn and (d) winter

area is the very different ice cover extent in the Arctic Ocean in the different GCMs, both in the baseline and future simulations (Collins *et al*., 2013, figs. 12.29–12.30).

For the lengths of the thermal summer and winter, the signal-to-noise ratio of the response is good: Over the majority of the area, the multi-model mean change is two- to three-fold compared to the inter-model *SD*. In contrast, for the intermediate seasons the signal is low apart from the Baltic countries where the signal-to-noise ratio is higher than 2.

The changes simulated by the individual GCMs at one example grid point in central Finland are given in Figure 5. The models agree on an earlier onset of the thermal spring and summer and a later onset of autumn and winter. The prolongation of the thermal summer and shortening of winter is likewise apparent in all the GCMs, but projections for the lengths of the intermediate thermal seasons are somewhat divergent.

3.2 | Relationship between modelled temperature increase and changes in thermal seasons

The scatter diagrams in Figure 5 depict the relationship between the simulated increase in the annual-mean temperature and time-mean change in the lengths (panels (a)-(d)) and onset times (panels (e)-(h)) of the thermal seasons across the ensemble of the 23 GCMs. At this example point, all the GCMs simulate higher mean temperatures for the future. Apart from the lengths of the intermediate seasons, the modelled annual-mean warming correlates well with changes in the onset times and lengths. Ignoring inter-model dependencies between the 23 GCMs ($\Rightarrow df = 21$), correlations higher than 0.41 are statistically significant at the 5% level; those above 0.52 at the 1% and above 0.64 at the 0.1% level.

The spatial distributions of the inter-model correlation coefficients between the annual-mean warming and shifts in the onset times (for all thermal seasons) and lengths (for summer and winter) are shown in Figure S7. In general, the correlations range from 0.8 to 0.9. However, the length and, in particular, onset time of the thermal summer in Lapland and the Scandinavian mountain area exhibits a far weaker dependency on the annual temperature increase. In these areas the thermal summer only lasts from late June to early August or is even shorter. Hence, the future lengthening of the thermal summer depends on the mean temperature increase taking place in the warmest months of the year alone. There are several models (e.g. CMCC-CM and BCC-CSM1-1) in which the simulated temperature increase is strongly seasonally dependent, that is, despite a major annual-mean warming the temperature response is fairly weak in the

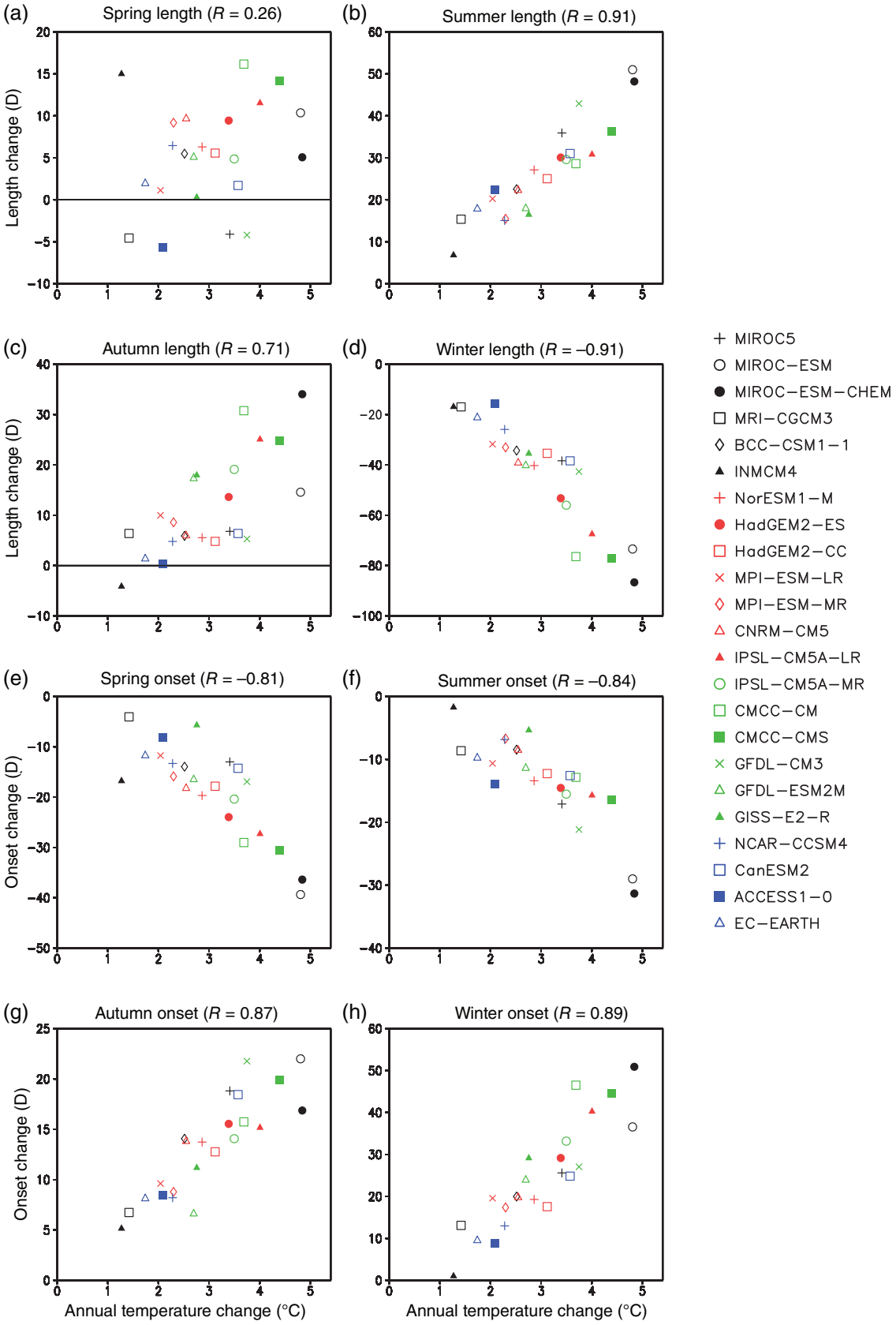

FIGURE 5 Scatter diagrams depicting the relation between changes in the annual-mean temperature (in °C) and the average length of the thermal (a) spring, (b) summer, (c) autumn and (d) winter (in days) in the ensemble of the 23 GCMs at 62.375°N, 27.625°E. Corresponding diagrams for the season onset times are given in panels (e)–(h). The inter-model correlation coefficients between the changes are shown above the panels. All changes are calculated for the period 2040–2069 (relative to 1971–2000) under the RCP4.5 scenario. For the symbols of the individual models, see the legend

summer months. Accordingly, in sub-arctic areas the annually averaged temperature increase is not an optimal predictor for the lengthening of the thermal summer.

The high correlation coefficients indicate that in most cases the modelled annual-mean temperature increase is a reasonably good proxy for the simulated changes in thermal seasons. To quantify this relationship, a linear regression forced to pass through the origin was fitted to the data:

$$\Delta X = \alpha \Delta T, \quad (1)$$

where ΔT is the model-simulated annual-mean temperature increase and ΔX the corresponding change in the onset time or length of a thermal season. Consequently, α reveals how many days earlier or later the onset of a thermal season will become per 1° of local warming; or how the season lengths respond to warming. A similar approach was used by Deng *et al*. (2018) to explain changes in the thermal growing season in China by annual-mean warming.

The spatial distributions of regression coefficients α are shown in Figure 6. Over the majority of the domain, a warming of 1°C advances the onset and delays the termination of thermal summers by 4–6 days, leading to an increase in the summer length by about 10 days (Figure 6b, c,e). In the areas of maritime climate, changes per 1°C of local warming are somewhat larger. For the thermal winter, an increase of temperature by 1°C leads to a shortening of about 10 days in the northern and eastern inland areas and more than 20 days in wide areas near the coasts of the Baltic Sea, in southern Sweden and on the coasts of Norway (panel f). The shortening tends to be somewhat stronger at the beginning than end of the winter (panels a and d). In Denmark where winters are short, warming does not lead to any substantial further reduction.

In most models, mean temperatures in northern Europe increase more strongly in winter than in summer (Kirtman *et al*., 2013, fig. 11.10). This is one explanation for the response being stronger in the thermal winter than summer lengths. Locally, extracting the temperature increase from selected calendar months rather than using the annual mean would evidently improve the explanatory power. Nevertheless, it would be difficult to select the months unambiguously for the entire domain since, for example, the thermal spring starts as early as in February in Denmark and not until May in Lapland (Figure 1a). Moreover, the onset times advance substantially in the course of the projection period. Consequently, to keep the statistical model straightforward, we have chosen to follow the approach of Deng *et al*. (2018) and use the annual-mean temperature change as the only independent variable.

In addition to the larger future increase in temperature in winter, the higher sensitivity of the length of the thermal winter compared to thermal summer can be explained by the typical annual cycle of the mean temperature (Figure 7). In low-lying areas south of 65°N, the thermal summer mainly starts in May and ends in September (Figure 1); these points of time are marked by B in Figure 7. In these times of the year, the time derivative representing the seasonal progress of the long-term mean temperature is large, and the projected general increase in mean temperatures leads to fairly modest shifts in the points of time when the 10°C temperature threshold is crossed (from B to B′). Conversely, in cold areas the corresponding crossing times fall at late June and early August (marked by A), that is, at the times of the year when the mean temperature alters fairly slowly as a function of season. This explains the relatively large sensitivity of the thermal summer length to warming over the Scandinavian mountains, for instance (Figure 6e).

The area with maximum sensitivity of the thermal winter length to warming lies in southern Sweden inland (Figure 6f). In that area the start of the thermal winter shifts from early December to early January and the end from early March to early February. In these months, the seasonal slope of the mean-temperature curve is very gentle, and increasing temperatures delay the onset and advance the termination of the thermal winter heavily (in Figure 7 from C to C′). Moreover, as will be discussed below, in this area years totally without a thermal winter are fairly infrequent in the baseline-period climate, unlike in Denmark and the southern coasts of Sweden.

Furthermore, in the areas of maritime climate seasonal contrasts in the mean temperature are weaker than in continental climatic areas, and the seasonal time derivative of temperature is thus universally less steep. Accordingly, there is a general tendency of the sensitivity of the thermal season lengths to increase towards the west and from continental to coastal regions (Figure 6).

4 | TEMPORAL VARIATIONS AND THE OCCURRENCE OF ANOMALOUS THERMAL SEASONS

4.1 | Projections for the temporal variability of the season lengths

*SD*s representing the temporal variability of the thermal season lengths are shown in Figures S8 (baseline period) and S9 (2040–2069 under RCP4.5) and the ratio of the two *SD*s in Figure 8. The *SD*s were first calculated separately for every GCM by treating the output of the parallel runs as a single sample. For example, if there are

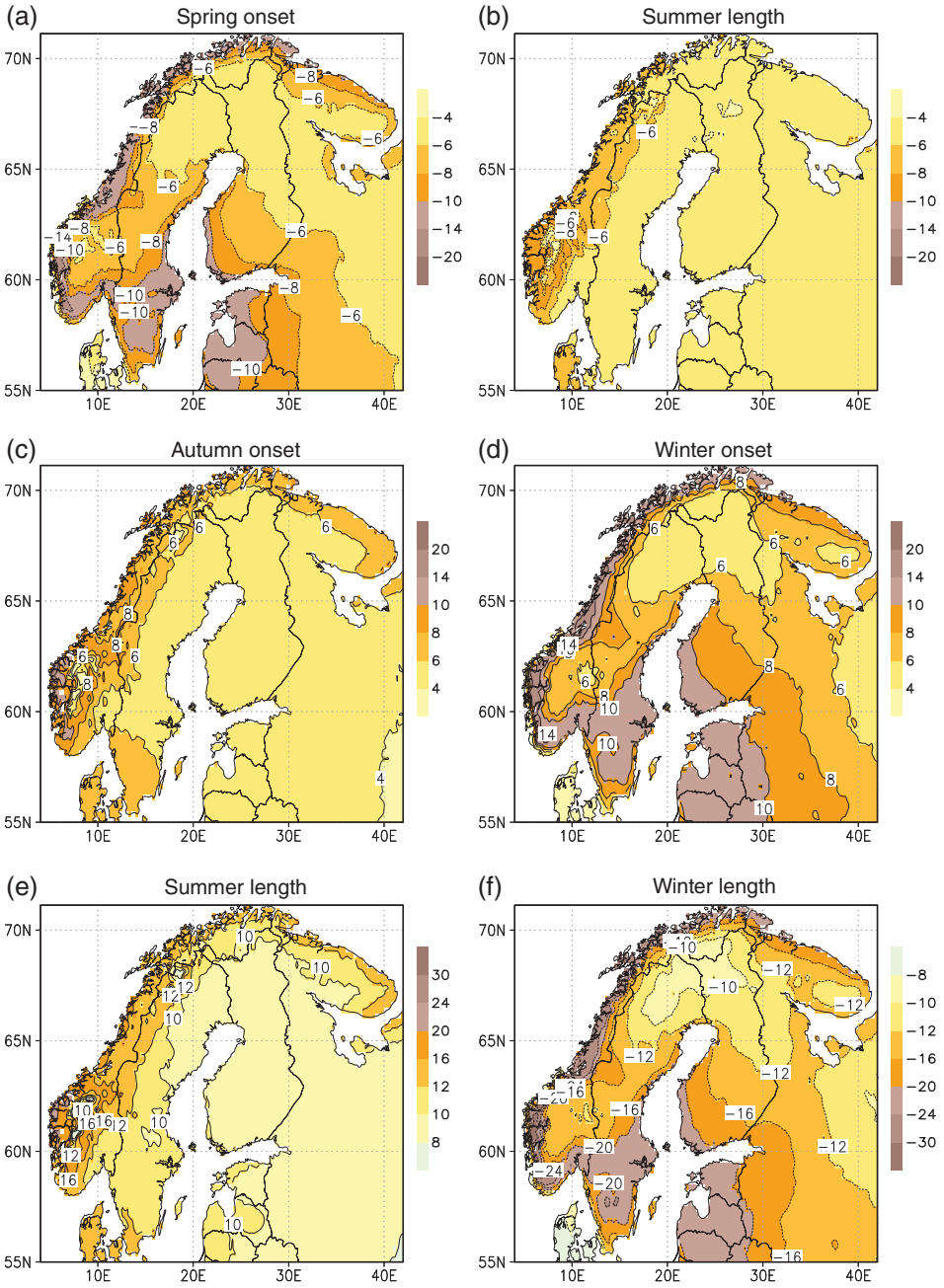

FIGURE 6 Regression coefficients between changes in the annual-mean temperature and the average onset date of the thermal (a) spring (b) summer, (c) autumn and (d) winter from the period 1971–2000 to 2040–2069 under RCP4.5, derived from the ensemble of the 23 GCMs; unit days/°C. The corresponding regression coefficients for the lengths of the thermal summer and winter are shown in panels (e) and (f). Note that the colour scale varies among the panels

three parallel runs, a 90-year-long time series was used for both 30-year periods. Finally, the multi-model mean estimate was calculated as the square root of the variance averaged over the 23 GCMs, by using a weighting identical to that in Section 3.1.

The temporal *SD*s of the season lengths (Figure S8) bear many similarities with the above-discussed sensitivity of the time-mean season lengths to changes in the mean temperatures (Figure 6). The interpretation of this finding is straightforward. When the start and end dates of a thermal season fall on such a stage of the seasonal cycle in which the slope of the mean temperature is gentle (e.g. points A and C in Figure 7), natural interannual variations in temperature lead to large fluctuations in the onset and termination dates.

As a consequence of the projected warming, the area where the start and end dates of the thermal winter are close to the bottom of the annual temperature cycle (Figure 7), but where a thermal winter with a nonzero length nevertheless occurs nearly every year, shifts northeastward (Figure S9D). Accordingly, interannual variations in the thermal winter length tend to be amplified remarkably in the zone extending from central Scandinavia through southern Finland to western Russia (Figure 8d). Meanwhile, variations are attenuated in southern Scandinavia and on the eastern coast of the

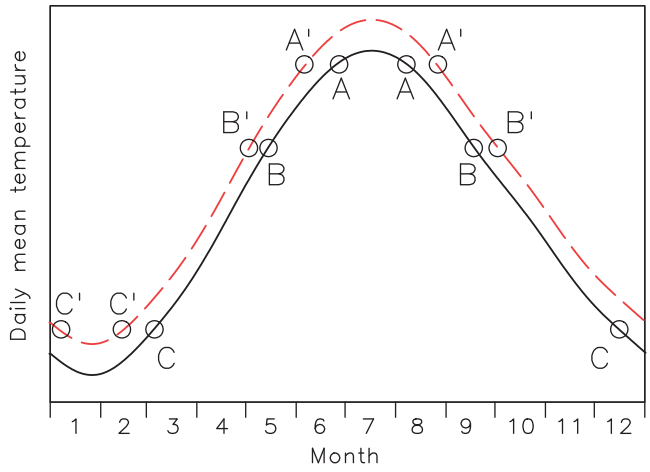

FIGURE 7 A schematic representation of the typical annual cycle of the mean temperature in the baseline climate (solid black curve) and a future climate with a constant seasonal warming (dashed curve); no scale for the temperature is given, since the temperatures are location-dependent. The letters A–C (A′–C′) refer to the baseline (future) onset and termination times of thermal seasons in the areas discussed in the text. Note that in the present work the onset and termination dates are actually derived from daily mean temperatures in each individual year rather than from the long-term means

Baltic Sea proper where years with a zero thermal winter length become prevalent (Figure 9b).

Conversely, temporal variations in the thermal summer length remain nearly unchanged outside of the coolest areas (Figure 8b), and there is no material change in the spread of the start and end dates either. Variations in the lengths of the intermediate thermal seasons thus mainly respond to changes in the fluctuations of the end of autumn (equivalent to the start of the thermal winter) and the beginning of spring. Therefore, changes in the variability of the thermal spring and autumn (Figure 8a, c) are qualitatively similar to those of the thermal winter, even though smaller in quantitative terms.

4.2 | Probabilities for the occurrence of anomalous thermal seasons

The occurrence of anomalous conditions is often of a greater practical importance than changes in the long-term mean state. In this section, the following events are discussed:

1. Years without a thermal winter or summer.
2. Anomalously short or long thermal winters.
3. Anomalously short or long thermal summers.
4. An anomalously early or late onset of the thermal spring.

As stated in Section 2, the probabilities have been derived from the entire ensemble of model runs and thus take into consideration both the influence of interannual variability and, for the projection periods, inter-model differences in the simulated climate change. For events 2–4, the anomalies have been determined relative to the local baseline-period means. In particular, a thermal season is regarded as very long if the length exceeds the baseline-period mean length by >20 days. Very short thermal seasons are defined analogously.

Geographical distributions for the probability of a missing thermal winter are depicted in Figure 9a,b. In 1971–2000, a thermal winter is experienced virtually every year (probability 98–100%) in the areas of cold or continental climate: north of 60°N apart from some coastal areas and in the entire Russian territory within the domain. On the eastern coast of the Baltic Sea and in the southern Scandinavian inland, a thermal winter occurs more often than in 4 years of five. In Denmark and on the coasts of southern Norway, winterless years constitute a majority. By mid-century, the probability of missing winters has increased considerably, particularly in southern Sweden and the Baltic countries (Figure 9b).

Temporal evolution of the probabilities of missing and very/moderately short and long thermal winters at four example locations is shown in Figure 10. In the baseline climate, approximately every second winter is longer/shorter than the average. By the period 2040–2069, at the three inland points the probability for longer-than-normal winters has fallen to ∼10% or below, and very long winters are extremely infrequent (Figure 10a,b,d). Correspondingly, the probability of an extremely short winter (very short or missing totally) is 60–75%. On the south-western coast of Sweden (Figure 10c), the length of the thermal winter varies greatly from year to year (Figure S8). At that point, the probabilities of both very short (including nonexistent) and very long winters are therefore larger than at the other three points.

Probabilities for thermal summers belonging to various categories are given in Figure 11. Years without a thermal summer only occur in Lapland, and they become increasingly infrequent in the future (Figure 11a). By mid-century, very long summers constitute a clear majority; their probability ranges from 60 to 70%, on the coasts of the Arctic Ocean even >80% (Figure 9d). Simultaneously, the probability of shorter-than-average summers has decreased below 10% (Figure 11).

Global warming leads to an advancement of thermal springs (Figure 12). At the three inland points

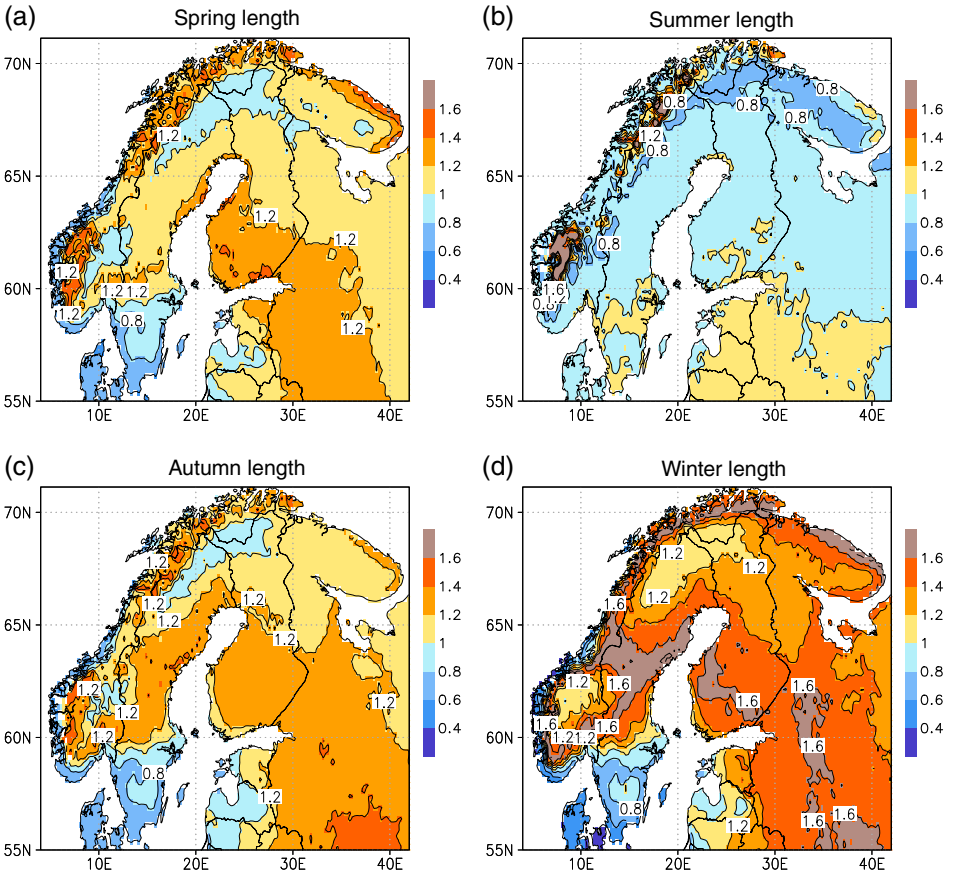

FIGURE 8 Multi-model mean responses of the interannual variability in the lengths of the thermal (a) spring, (b) summer, (c) autumn and (d) winter; the ratio of the temporal *SD* calculated for the period 2040–2069 under RCP4.5 to the *SD* of 1971–2000

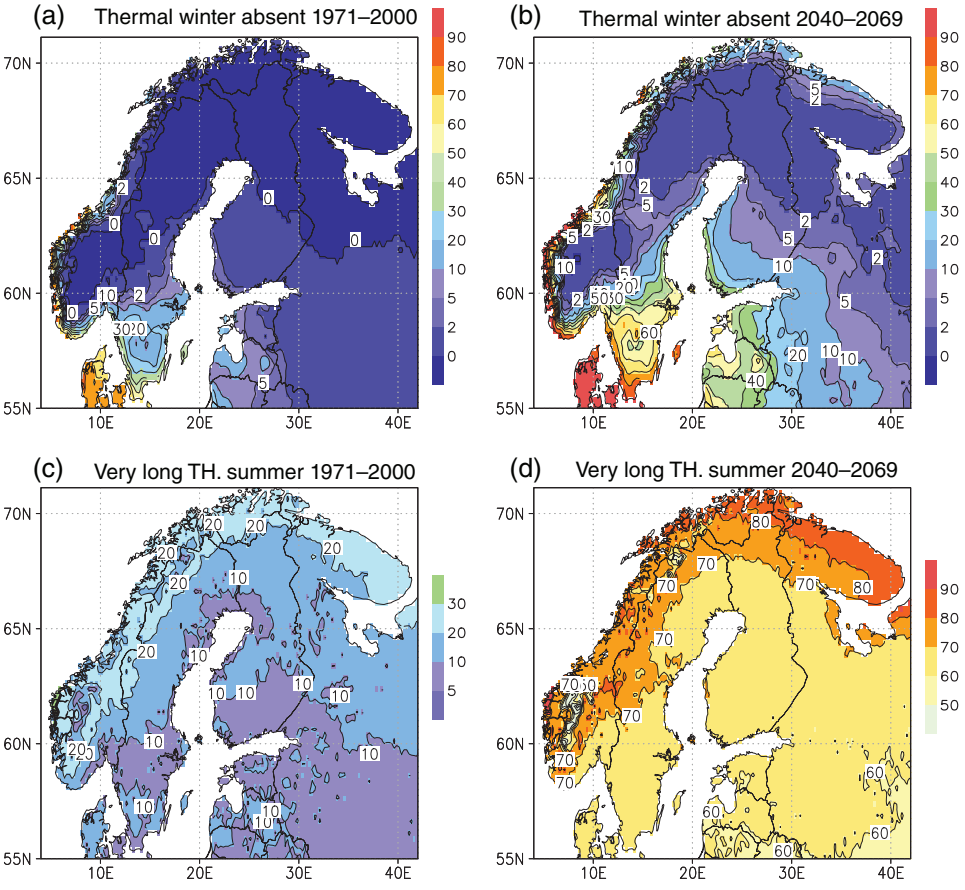

FIGURE 9 Model-derived annual probabilities (in %) for the occurrence of a year without a thermal winter in (a) 1971–2000 and (b) 2040–2069 under RCP4.5. Corresponding probabilities for the thermal summer being more than 20 days longer than the baseline-period mean are given in panels (c) and (d)

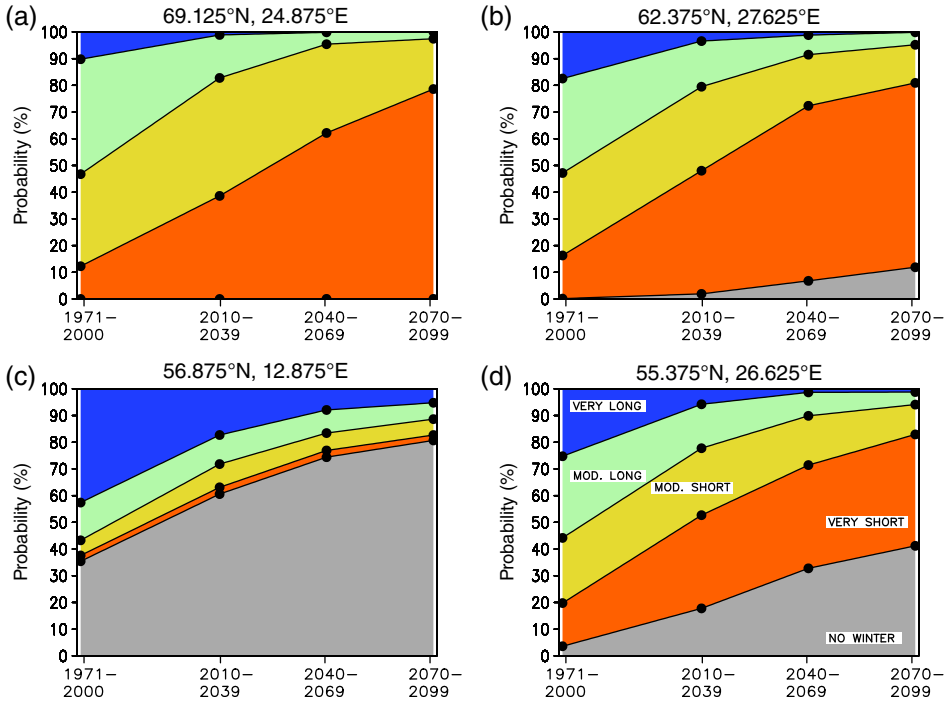

FIGURE 10 Model-derived annual probabilities under RCP4.5 (in %) for the absence of a thermal winter ('no winter') and the thermal winter being more than 20 days shorter ('very short'), 0–20 days shorter ('moderately short'), 0–20 days longer ('moderately long') or more than 20 days longer ('very long') than the local baseline-period mean. The probabilities are determined for the four periods marked in the figures and interpolated linearly between them. The four grid points considered are the same as in Figure 3. The average length of the thermal winter in 1971–2000 is (a) 212.2, (b) 149.3, (c) 58.1 and (d) 112.1 days

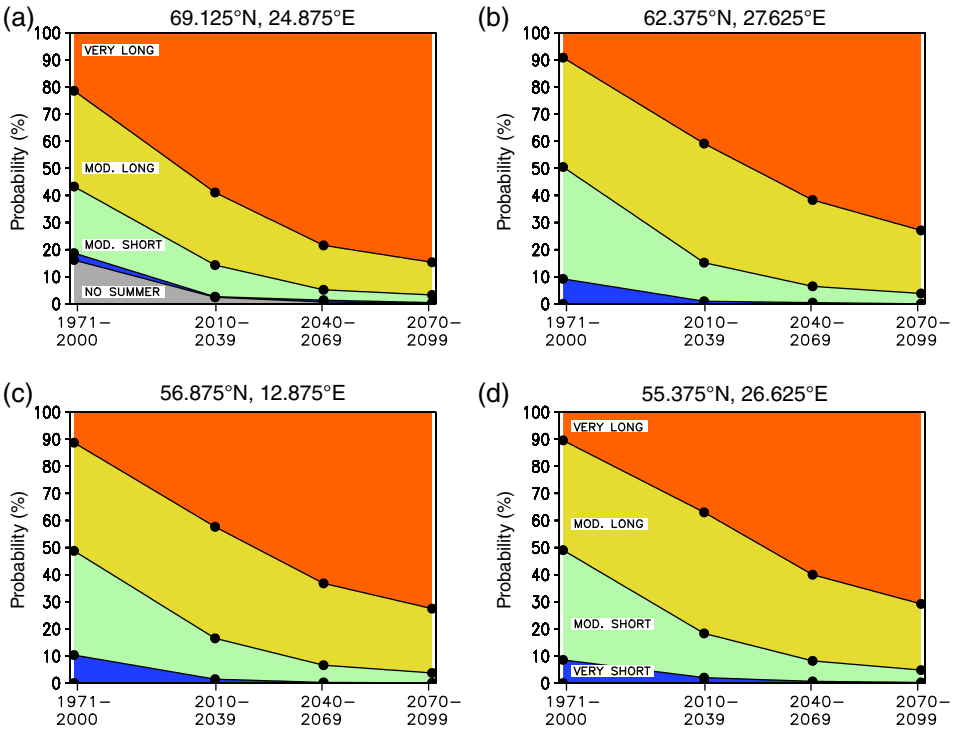

FIGURE 11 Model-derived annual probabilities under RCP4.5 (in %) for the absence of a thermal summer ('no summer') and the thermal summer being >20 days shorter ('very short'), 0–20 days shorter ('moderately short'), 0–20 days longer ('moderately long') or >20 days longer ('very long') than the baseline-period mean. The average length of the thermal summer in 1971–2000 is (a) 45.7, (b) 111.1, (c) 137.8 and (d) 141.8 days. For further information, see the caption of Figure 10

(Figure 12a,b,d), during the baseline period the probabilities of very early and very late springs (the start date deviating by more than 10 days from the 30-year average) are both about 20–30%. In 2040–2069, very late springs are highly unlikely, whereas very early springs have a probability of 60–70%. At the coastal point examined in Figure 12c, interannual variations in the spring onset times are larger than at the other locations, increasing the proportion of anomalous thermal springs.

In the late-21st century, probabilities of anomalously short winters, long summers and early springs continue to increase, even though less rapidly than during the first half of the century.

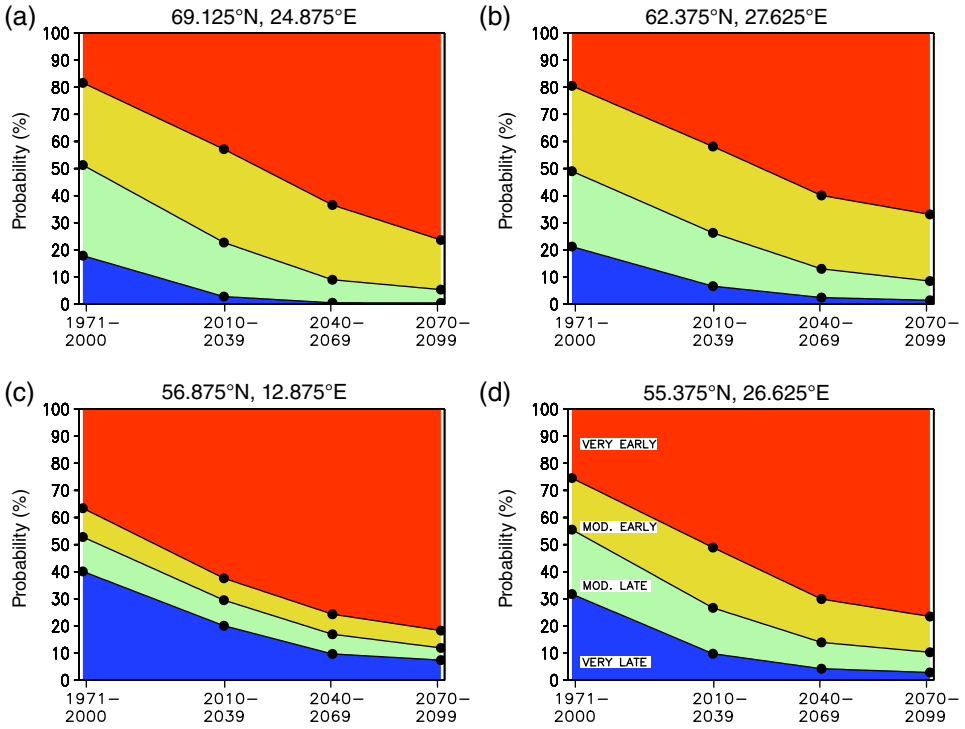

FIGURE 12 Model-derived annual probabilities under RCP4.5 (in %) for the thermal spring starting >10 days earlier ('very early'), 0–10 days earlier ('moderately early'), 0–10 days later ('moderately late') or >10 days later ('very late') than during the baseline period (1971–2000) on average. The mean Julian onset dates in 1971–2000 are (a) 127.1, (b) 95.4, (c) 54.8 and (d) 77.0. For further information, see the caption of Figure 10

5 | IMPLICATIONS

Short thermal winters act to reduce the ice period in northern European watersheds and the Baltic Sea (Jylhä *et al.*, 2014; Luomaranta *et al.*, 2014). The snow season shortens as well, and snow cover is projected to be thinner (Luomaranta *et al.*, 2019). In conjunction with the advancement of the thermal springs, this leads to earlier and weaker spring floods in rivers while winter discharges increase (Olsson *et al.*, 2015). These changes affect the preconditions of hydropower production.

As the thermal spring lengthens, successive phases of vernal phenology follow one another in a slower pace (Contosta *et al.*, 2017). Many birds are able to adjust the migration times to earlier springs (e.g. Vaitkuvienė *et al.*, 2015). In the future, the early but slowly evolving thermal springs affect the synchrony of nesting with the availability of food; the influence may be either negative or positive, depending on the bird species (Laaksonen *et al.*, 2006; Vatka *et al.*, 2011, and references therein).

Saimaa ringed seal is a critically endangered endemic species that only lives in one inland watershed in eastern Finland. The seals breed on the lake ice and build the lairs in snow banks (Auttila *et al.*, 2014). The shortening and, in the long run, potential disappearance of thermal winters hampers the reproduction of the seals, increasing the risk of extinction of this species despite active conservation efforts.

Some fish species benefit and others suffer from the ongoing shifts of the thermal seasons. The growth of pikeperches is well explained by the thermal summer in water, that is, the temperature sum above +10°C calculated from the water temperatures; the higher the temperature sum, the larger the annual length increment (Lappalainen *et al.*, 2009). In contrast, for cold-water fishes such as trouts and salmons, the long and warm summers have a negative impact (Clews *et al.*, 2010).

For reindeer husbandry, changes in the lengths of the thermal seasons likewise have both beneficial and adverse impacts (Turunen *et al.*, 2016). Due to the shortening of thermal winters, extremely deep snow cover in winter and a late snow-melt in spring, both being detrimental to reindeer well-being, become less frequent. Conversely, in mild winters freeze and thaw tend to alternate, forming ice layers within the snow pack and on the ground. Hard ice layers hamper digging of forage below the snow. Moreover, reindeer is adapted to sub-arctic climate conditions and therefore suffers from the increasingly numerous heat waves during the longer thermal summers. In particular, the occurrence of successive warm summers exposes reindeers to parasite epidemics (Laaksonen *et al.*, 2010).

In agriculture, the long thermal summers enable cultivation of heat-demanding crop species and varieties, and meanwhile the short winters favour winter-sown crops (Peltonen-Sainio *et al.*, 2009). For example, maize is not sown until the mean temperature reaches +10°C (Olesen *et al.*, 2012); that is, in the beginning of the thermal summer. Owing to the small amount of light, in northern European conditions a very late end of the

thermal summer engenders less benefit than an early onset. Moreover, in late autumn excessive moisture tends to complicate crop harvesting (Peltonen-Sainio *et al*., 2009). Conversely, the long thermal autumns and short winters contribute to the over-wintering of frost-sensitive perennial plants, such as fruit trees (Laapas *et al*., 2012).

In wild plants, the earlier onset of thermal springs does not necessarily increase the total annual growth, since water resources in the soil may then be depleted earlier, resulting in drought stress (Buermann *et al*., 2018). Even so, according to Holmberg *et al*. (2019) warming is likely to increase the carbon sink in boreal forests; particularly the tree biomass (Sievänen *et al*., 2014). However, the long-lasting thermal autumns act to enhance the total ecosystem respiration more than photosynthesis, which turns the carbon balance more negative in that season (Vesala *et al*., 2010).

In the boreal zone, the annual phenology of trees is primarily controlled by temperature conditions. In autumn after the growing period, the trees are in dormancy; thereafter, exposure to chilling induced by cool temperatures gradually breaks the dormancy, leading trees into the ecodormancy stage (Linkosalo *et al*., 2006; Piao *et al*., 2019). In the following spring, an adequate temperature accumulation is needed to start the growth. However, if there has been insufficient chilling during the preceding autumn and winter to break the dormancy, the vernal start of the growth may be delayed (Piao *et al*., 2019, and references therein). Accordingly, it is possible that in the future the start of the growth in trees does not advance as much as the onset times of the thermal spring and summer become earlier. Moreover, trees respond more strongly to increasing day-time than night-time temperatures (Piao *et al*., 2019). This point is not taken into account in the present projections of the thermal seasons since the seasons are inferred, by definition, exclusively from the daily-mean temperatures. In autumn, the termination of the growing period is primarily influenced by the photoperiod rather than temperature (Piao *et al*., 2019). Accordingly, the growth of forests is not likely to benefit significantly from the later end of the thermal summer and autumn.

The prolongation of thermal summers acts to increase the number of days with a high risk of wildfire ignition (Lehtonen *et al*., 2014). The shortening of thermal winters deteriorates the preconditions of timber harvesting and transportation of timber in forest truck roads, since the lack of ground frost weakens ground-bearing capacity (Lehtonen *et al*., 2019).

Owing to the reduction of the length of thermal winters, the season of cross-country and alpine skiing tourism becomes shorter (Damm *et al*., 2017). The prolongation of thermal summers makes the heating season in buildings shorter whereas the cooling season lengthens (Jylhä *et al*., 2015; Spinoni *et al*., 2018).

6 | CONCLUDING REMARKS

In this study, the lengths of the thermal seasons have been derived from bias-corrected output data extracted from 23 CMIP5 GCMs. Most emphasis is given to the mid-century climate (years 2040–2069) under RCP4.5, compared to the baseline period 1971–2000. According to the multi-model mean projection, the average thermal summer lengthens by about 2 weeks at both ends. In subarctic areas, the prolongation is somewhat more pronounced. Correspondingly, in boreal areas the thermal winter is projected to shorten by 2–3 weeks at both ends, in areas of maritime climate even more. The inter-model agreement on the direction of the changes is good. Since thermal winters shorten over the majority of the domain more strongly than summers lengthen, the thermal spring and autumn generally tend to be prolonged.

In the model ensemble, there is a strong linear dependence between the simulated annual-mean temperature increase and modelled changes in the onset times of the thermal seasons. Over the majority of the domain, a warming of 1°C acts to prolong thermal summers by about 10 days and to reduce thermal winters by 10–24 days. The response is strongest in the areas where climate is maritime or the start and end dates of the thermal summer (winter) fall close to the maximum (minimum) point of the annual temperature cycle. As all the GCMs explored simulate higher annual-mean temperatures for the future, there is a high inter-model agreement on the lengthening of the thermal summer and shortening of winter as well.

In addition to the time-mean changes, we explored the occurrence of such thermal seasons that are anomalous according to the baseline-climate standards. By mid-century, over the majority of the domain the probability for the occurrence of very long summers (more than 20 days longer than the baseline-period mean) and very early springs (the onset time more than 10 days earlier) has reached 60–70%. The probability for a very short thermal winter (anomaly >20 days or missing totally) is generally somewhat larger, 65–75%. This is in concordance with the tendency of the models to simulate largest temperature increases for the cold season.

As discussed in Section 5, changes in the timing and lengths of the thermal seasons have numerous impacts on nature and human society, including biodiversity, water resources, agriculture, tourism and forestry. For example, the growth of forest is likely to accelerate, but this benefit is counteracted by a potential shortage of

water and an increasing risk for forest fires. Shortening of thermal winters reduces the soil frost period, which acts to complicate timber harvesting in forests.

All the projections discussed in this article are founded on the RCP4.5 scenario, in addition to which some results for RCP8.5 are given for comparison in the supplement. Under RCP4.5, the global mean temperature increases by about 2°C from the preindustrial era to mid-century. If global climate policy proves to be successful, the ultimate equilibrium-state warming may even be weaker, resulting in somewhat smaller changes in the thermal seasons than are reported here.

ACKNOWLEDGEMENTS

This work was supported financially by the Academy of Finland through the FORBIO and SOMPA projects of the Strategic Research Council (decisions 314224 and 312932). The CMIP5 GCM data were downloaded from the Earth System Grid Federation (ESGF) data archive (http://esgf-node.llnl.gov/search/cmip5). The modelling groups are acknowledged for making their model output available through ESGF. Ari Venäläinen is thanked for assistance in searching for references and both official reviewers for their comments on the first version of the manuscript.

ORCID

Kimmo Ruosteenoja https://orcid.org/0000-0002-4370-0782

REFERENCES

Allen, M.J. and Sheridan, S.C. (2016) Evaluating changes in season length, onset, and end dates across the United States (1948–2012). *International Journal of Climatology*, 36, 1268–1277. https://doi.org/10.1002/joc.4422.

Auttila, M., Niemi, M., Skrzypczak, T., Viljanen, M. and Kunnasranta, M. (2014) Estimating and mitigating perinatal mortality in the endangered Saimaa ringed seal (*Phoca hispida saimensis*) in a changing climate. *Annales Zoologici Fennici*, 51, 526–534. https://doi.org/10.5735/086.051.0601.

Buermann, W., Forkel, M., O'Sullivan, M., Sitch, S., Friedlingstein, P., Haverd, V., Jain, A.K., Kato, E., Kautz, M., Lienert, S., Lombardozzi, D., Nabel, J.E.M.S., Tian, H., Wiltshire, A.J., Zhu, D., Smith, W.K. and Richardson, A.D. (2018) Widespread seasonal compensation effects of spring warming on northern plant productivity. *Nature*, 562, 110–114. https://doi.org/10.1038/s41586-018-0555-7.

Clews, E., Durance, I., Vaughan, I.P. and Ormerod, S.J. (2010) Juvenile salmonid populations in a temperate river system track synoptic trends in climate. *Global Change Biology*, 16, 3271–3283. https://doi.org/10.1111/j.1365-2486.2010.02211.x.

Collins, M., Knutti, R., Arblaster, J., Dufresne, J.L., Fichefet, T., Friedlingstein, P., Gao, X., Gutowski, W., Johns, T., Krinner, G., Shongwe, M., Tebaldi, C., Weaver, A. and Wehner, M. (2013) Long-term climate change: projections, commitments and irreversibility. In: Stocker, T.F., Qin, D., Plattner, G.K., Tignor, M., Allen, S.K., Boschung, J., Nauels, A., Xia, Y., Bex, V. and Midgley, P.M. (Eds.) *Climate Change 2013: The Physical Science Basis. Contribution of Working Group I to the Fifth Assessment Report of the Intergovernmental Panel on Climate Change*. [Chapter 12]. Cambridge, United Kingdom and New York, USA: Cambridge University Press, pp. 1029–1136.

Contosta, A.R., Adolph, A., Burchsted, D., Burakowski, E., Green, M., Guerra, D., Albert, M., Dibb, J., Martin, M., McDowell, W.H., Routhier, M., Wake, C., Whitaker, R. and Wollheim, W. (2017) A longer vernal window: the role of winter coldness and snowpack in driving spring transitions and lags. *Global Change Biology*, 23, 1610–1625. https://doi.org/10.1111/gcb.13517.

Czernecki, B. and Miętus, M. (2017) The thermal seasons variability in Poland, 1951–2010. *Theoretical and Applied Climatology*, 127, 481–493. https://doi.org/10.1007/s00704-015-1647-z.

Damm, A., Greuell, W., Landgren, O. and Prettenthaler, F. (2017) Impacts of +2°C global warming on winter tourism demand in Europe. *Climate Services*, 7, 31–46. https://doi.org/10.1016/j.cliser.2016.07.003.

Deng, H., Yin, Y. and Wu, S. (2018) Divergent responses of thermal growing degree-days and season to projected warming over China. *International Journal of Climatology*, 38, 5605–5618. https://doi.org/10.1002/joc.5766.

Engen-Skaugen, T. and Tveito, O.E. (2004) Growing-season and degree-day scenario in Norway for 2021–2050. *Climate Research*, 26, 221–232.

Fernández-Long, M.E., Müller, G.V., Beltrán-Przekurat, A. and Scarpati, O.E. (2013) Long-term and recent changes in temperature-based agroclimatic indices in Argentina. *International Journal of Climatology*, 33, 1673–1686. https://doi.org/10.1002/joc.3541.

Haylock, M.R., Hofstra, N., Klein Tank, A.M.G., Klok, E.J., Jones, P.D. and New, M. (2008) A European daily high-resolution gridded dataset of surface temperature and precipitation for 1950–2006. *Journal of Geophysical Research*, 113(D20), D20119. https://doi.org/10.1029/2008JD010201.

Holmberg, M., Aalto, T., Akujärvi, A., Arslan, A.N., Bergström, I., Böttcher, K., Lahtinen, I., Mäkelä, A., Markkanen, T., Minunno, F., Peltoniemi, M., Rankinen, K., Vihervaara, P. and Forsius, M. (2019) Ecosystem services related to carbon cycling – modeling present and future impacts in boreal forests. *Frontiers in Plant Science*, 10, 343. https://doi.org/10.3389/fpls.2019.00343.

Jaagus, J., Truu, J., Ahas, R. and Aasa, A. (2003) Spatial and temporal variability of climatic seasons on the east European plain in relation to large-scale atmospheric circulation. *Climate Research*, 23, 111–129.

Jylhä, K., Jokisalo, J., Ruosteenoja, K., Pilli-Sihvola, K., Kalamees, T., Seitola, T., Mäkelä, H.M., Hyvönen, R., Laapas, M. and Drebs, A. (2015) Energy demand for the heating and cooling of residental houses in Finland in a changing climate. *Energy and Buildings*, 99, 104–116. https://doi.org/10.1016/j.enbuild.2015.04.001.

Jylhä, K., Laapas, M., Ruosteenoja, K., Arvola, L., Drebs, A., Kersalo, J., Saku, S., Gregow, H., Hannula, H.R. and Pirinen, P. (2014) Climate variability and trends in the Valkea-Kotinen region, southern Finland: comparisons between the past, current and projected climates. *Boreal Environment Research*, 19 (Supplement A), 4–30.

Kirtman, B., Power, S., Adedoyin, J., Boer, G., Bojariu, R., Camilloni, I., Doblas-Reyes, F., Fiore, A., Kimoto, M., Meehl, G., Prather, M., Sarr, A., Schär, C., Sutton, R., van Oldenborgh, G., Vecchi, G. and Wang, H. (2013) Near-term climate change: projections and predictability. In: Stocker, T.F., Qin, D., Plattner, G. K., Tignor, M., Allen, S.K., Boschung, J., Nauels, A., Xia, Y., Bex, V. and Midgley, P.M. (Eds.) *Climate Change 2013: The Physical Science Basis. Contribution of Working Group I to the Fifth Assessment Report of the Intergovernmental Panel on Climate Change*. [Chapter 11]. Cambridge, United Kingdom and New York, USA: Cambridge University Press, pp. 953–1028.

Kull, A., Kull, A., Jaagus, J., Kuusemets, V. and Mander, Ü. (2008) The effects of fluctuating climatic conditions and weather events on nutrient dynamics in a narrow mosaic riparian peatland. *Boreal Environment Research*, 13, 243–263.

Laaksonen, S., Pusenius, J., Kumpula, J., Venäläinen, A., Kortet, R., Oksanen, A. and Hoberg, E. (2010) Climate change promotes the emergence of serious disease outbreaks of filarioid nematodes. *EcoHealth*, 7, 7–13. https://doi.org/10.1007/s10393-010-0308-z.

Laaksonen, T., Ahola, M., Eeva, T., Väisänen, R.A. and Lehikoinen, E. (2006) Climate change, migratory connectivity and changes in laying date and clutch size of the pied flycatcher. *Oikos*, 114, 277–290.

Laapas, M., Jylhä, K. and Tuomenvirta, H. (2012) Climate change and future overwintering conditions of horticular woody-plants in Finland. *Boreal Environment Research*, 17, 31–45.

Lappalainen, J., Milardi, M., Nyberg, K. and Venäläinen, A. (2009) Effects of water temperature on year-class strengths and growth patterns of pikeperch (*Sander lucioperca* (L.)) in the brackish Baltic Sea. *Aquatic Ecology*, 43, 181–191. https://doi.org/10.1007/s10452-007-9150-y.

Leduc, M., Laprise, R., de Elía, R. and Šeparović, L. (2016) Is institutional democracy a good proxy for model independence? *Journal of Climate*, 29, 8301–8316. https://doi.org/10.1175/JCLI-D-15-0761.1.

Lehtonen, I., Ruosteenoja, K., Venäläinen, A. and Gregow, H. (2014) The projected 21st century forest-fire risk in Finland under different greenhouse gas scenarios. *Boreal Environment Research*, 19, 127–139.

Lehtonen, I., Venäläinen, A., Kämäräinen, M., Asikainen, A., Laitila, J., Anttila, P. and Peltola, H. (2019) Projected decrease in wintertime bearing capacity on different forest and soil types in Finland under a warming climate. *Hydrology and Earth System Sciences*, 23, 1611–1631. https://doi.org/10.5194/hess-23-1611-2019.

Linkosalo, T., Häkkinen, R. and Hänninen, H. (2006) Models of the spring phenology of boreal and temperate trees: is there something missing? *Tree Physiology*, 26, 1165–1172. https://doi.org/10.1093/treephys/26.9.1165.

Luomaranta, A., Aalto, J. and Jylhä, K. (2019) Snow cover trends in Finland over 1961–2014 based on gridded snow depth observations. *International Journal of Climatology*, 39, 3147–3159. https://doi.org/10.1002/joc.6007.

Luomaranta, A., Ruosteenoja, K., Jylhä, K., Gregow, H., Haapala, J. and Laaksonen, A. (2014) Multimodel estimates of the changes in the Baltic Sea ice cover during the present century. *Tellus A*, 66, 22617. https://doi.org/10.3402/tellusa.v66.22617.

Olesen, J., Børgesen, C., Elsgaard, L., Palosuo, T., Rötter, R., Skjelvåg, A., Peltonen-Sainio, P., Börjesson, T., Trnka, M., Ewert, F., Siebert, S., Brisson, N., Eitzinger, J., van Asselt, E., Oberforster, M. and van der Fels-Klerx, H. (2012) Changes in time of sowing, flowering and maturity of cereals in Europe under climate change. *Food Additives & Contaminants: Part A*, 29, 1527–1542. https://doi.org/10.1080/19440049.2012.712060.

Olsson, T., Jakkila, J., Veijalainen, N., Backman, L., Kaurola, J. and Vehviläinen, B. (2015) Impacts of climate change on temperature, precipitation and hydrology in Finland – studies using bias corrected regional climate model data. *Hydrology and Earth System Sciences*, 19, 3217–3238. https://doi.org/10.5194/hess-19-3217-2015.

Park, B.J., Kim, Y.H., Min, S.K. and Lim, E.P. (2018) Anthropogenic and natural contributions to the lengthening of the summer season in the Northern Hemisphere. *Journal of Climate*, 31, 6803–6819. https://doi.org/10.1175/JCLI-D-17-0643.1.

Peltonen-Sainio, P., Jauhiainen, L., Hakala, K. and Ojanen, H. (2009) Climate change and prolongation of growing season: changes in regional potential for field crop production in Finland. *Agricultural and Food Science*, 18, 171–190.

Peña-Ortiz, C., Barriopedro, D. and García-Herrera, R. (2015) Multidecadal variability of the summer length in Europe. *Journal of Climate*, 28, 5375–5388. https://doi.org/10.1175/JCLI-D-14-00429.1.

Piao, S., Liu, Q., Chen, A., Janssens, I.A., Fu, Y., Dai, J., Liu, L., Lian, X., Shen, M. and Zhu, X. (2019) Plant phenology and global climate change: current progresses and challenges. *Global Change Biology*, 25, 1922–1940. https://doi.org/10.1111/gcb.14619.

Przybylak, R. and Wyszyński, P. (2017) Air temperature in Novaya Zemlya archipelago and Vaygach Island from 1832 to 1920 in the light of early instrumental data. *International Journal of Climatology*, 37, 3491–3508. https://doi.org/10.1002/joc.4934.

Räisänen, J. and Räty, O. (2013) Projections of daily mean temperature variability in the future: cross-validation tests with ENSEMBLES regional climate simulations. *Climate Dynamics*, 41, 1553–1568. https://doi.org/10.1007/s00382-012-1515-9.

Ruosteenoja, K., Räisänen, J. and Pirinen, P. (2011) Projected changes in thermal seasons and the growing season in Finland. *International Journal of Climatology*, 31, 1473–1487. https://doi.org/10.1002/joc.2171.

Ruosteenoja, K., Räisänen, J., Venäläinen, A. and Kämäräinen, M. (2016) Projections for the duration and degree days of the thermal growing season in Europe derived from CMIP5 model output. *International Journal of Climatology*, 36, 3039–3055. https://doi.org/10.1002/joc.4535.

Saue, T. and Käremaa, K. (2015) Lengthening of the thermal growing season due climate change in Estonia. In: Šiška, B., Nejedlík, P., and Eliášová, M. (Eds.) *Towards Climatic Services*, Nitra, Slovakia, 15–18 September 2015. Nitra, Slovakia: Slovak University of Agriculture.

Sievänen, R., Salminen, O., Lehtonen, A., Ojanen, P., Liski, J., Ruosteenoja, K. and Tuomi, M. (2014) Carbon stock changes of forest land in Finland under different levels of wood use and climate change. *Annals of Forest Science*, 71, 255–265. https://doi.org/10.1007/s13595-013-0295-7.

Spinoni, J., Vogt, J.V., Barbosa, P., Dosio, A., McCormick, N., Bigano, A. and Füssel, H.M. (2018) Changes of heating and cooling degree-days in Europe from 1981 to 2100. *International Journal of Climatology*, 38, e191–e208. https://doi.org/10.1002/joc.5362.

Tian, Z., Yang, X., Sun, L., Fischer, G., Liang, Z. and Pan, J. (2014) Agroclimatic conditions in China under climate change scenarios projected from regional climate models. *International Journal of Climatology*, 34, 2988–3000. https://doi.org/10.1002/joc.3892.

Trnka, M., Eitzinger, J., Semerádová, D., Hlavinka, P., Balek, J., Dubrovský, M., Kubu, G., Štěpánek, P., Thaler, S., Možný, M. and žalud, Z. (2011) Expected changes in agroclimatic conditions in Central Europe. *Climatic Change*, 108, 261–289. https://doi.org/10.1007/s10584-011-0025-9.

Turunen, M., Rasmus, S., Bavay, M., Ruosteenoja, K. and Heiskanen, J. (2016) Coping with difficult weather and snow conditions: reindeer herders' views on climate change impacts and coping strategies. *Climate Risk Management*, 11, 15–36. https://doi.org/10.1016/j.crm.2016.01.002.

Vaitkuviené, D., Dagys, M., Bartkevičiené, G. and Romanovskaja, D. (2015) The effect of weather variables on the white stork (*Ciconia ciconia*) spring migration phenology. *Ornis Fennica*, 92, 43–52.

van Vuuren, D.P., Edmonds, J., Kainuma, M., Riahi, K., Thomson, A., Hibbard, K., Hurtt, G.C., Kram, T., Krey, V., Lamarque, J.F., Masui, T., Meinshausen, M., Nakicenovic, N., Smith, S.J. and Rose, S.K. (2011) The representative concentration pathways: an overview. *Climatic Change*, 109, 5–31. https://doi.org/10.1007/s10584-011-0148-z.

Vatka, E., Orell, M. and Rytkönen, S. (2011) Warming climate advances breeding and improves synchrony of food demand and food availability in a boreal passerine. *Global Change Biology*, 17, 3002–3009. https://doi.org/10.1111/j.1365-2486.2011.02430.x.

Vesala, T., Launiainen, S., Kolari, P., Pumpanen, J., Sevanto, S., Hari, P., Nikinmaa, E., Kaski, P., Mannila, H., Ukkonen, E., Piao, S. and Ciais, P. (2010) Autumn temperature and carbon balance of a boreal scots pine forest in southern Finland. *Biogeosciences*, 7, 163–176. https://doi.org/10.5194/bg-7-163-2010.

WMO. (1989) *Calculation of Monthly and Annual 30-Year Standard Normals*. Geneva: World Meteorological Organization WCDP No. 10, WMO-TD/No. 341.

Yang, X., Tian, Z. and Chen, B. (2013) Thermal growing season trends in East China, with emphasis on urbanization effects. *International Journal of Climatology*, 33, 2402–2412. https://doi.org/10.1002/joc.3590.

Zhou, B., Zhai, P., Chen, Y. and Yu, R. (2018) Projected changes of thermal growing season over northern Eurasia in a 1.5°C and 2°C warming world. *Environmental Research Letters*, 13, 035004. https://doi.org/10.1088/1748-9326/aaa6dc.

SUPPORTING INFORMATION

Additional supporting information may be found online in the Supporting Information section at the end of this article.

How to cite this article: Ruosteenoja K, Markkanen T, Räisänen J. Thermal seasons in northern Europe in projected future climate. *Int J Climatol*. 2020;40:4444–4462. https://doi.org/10.1002/joc.6466